Optical Properties of Mesoporous Gold Films

A. I. Maaroof, M. B. Cortie*, G.B. Smith
Institute of Nanoscale Technology and Department of Applied Physics, University of Technology, Sydney PO Box 123 Broadway NSW 2007
*Corresponding author: michael.cortie@uts.edu.au (Michael B. Cortie)
PACS code: **78.20**.Ci , 78.55.Mb, 78.66.-W, 68.55.-a, 68.55.Nq

Abstract
Mesoporous gold thin films on glass substrates were fabricated by sputtering of $AuAl_2$ precursor films followed by a de-alloying etch. The resulting sponge-like Au films have very high internal surface area due to nanoscale pores and channels. Scattering is not significant and the optical properties for such nanostructured films were examined using ellipsometry and spectrophotometry. The complex refractive indices of the optically equivalent uniform smooth layer satisfy Kramers-Kronig (K-K) self-consistency but have unusual dispersion relations and magnitudes for a film containing the amount of noble metal present. The reflectance at infrared wavelengths is neither metal nor insulator like, and the indices have unique dispersion curves.

I. Introduction

Mesoporous gold powder can be produced by de-alloying $AuAl_2$ [1] and thin films of $AuAl_2$ have been studied for decorative uses on account of their bright purple colour [2] . However de-alloyed thin films have not been studied in any detail until recently [3], and to our knowledge no detailed analysis of their optical properties have been published. Thin mesoporous gold films have unique surface and internal nanostructure whose properties have recently inspired interest because of their wide range of potential applications including sensors and ultra-capacitors [3]. Internal surface areas are large as a result of many nanoscale pores and channels. A study of the optical properties of such nanostructured films is of fundamental interest for understanding how light interacts with nano-porous spongy structures. In general the gold in nanoscale coatings either percolates or is very closely packed. Thus surface plasmons, and possibly surface plasmon resonant effects, are expected to play a key role given the large surface area of metal and the metal backbone of the nanostructure. The topological complexity of the nanovoid network is also expected to be a major influence. Once the optical response, which includes unusual dispersion relations, is better understood new optical engineering possibilities may arise.
Many of these layers do not significantly scatter plane waves because their inhomogeneities are at a scale that is well below the wavelength. It is then possible to represent them by an optically equivalent layer, which is smooth, and of the same thickness as the porous layer [4]. This layer has a complex refractive index of the form $N^*(\lambda)=n^*(\lambda)+ik^*(\lambda)$, which is a useful parameter to study as it yields insights into the overall interactions of light with such mesoporous metal nanostructures, when considered

as a homogeneous optical layer. For instance do the relative magnitudes of n^*, k^* still represent a uniform plasmonic system? The complex dielectric function of the optically equivalent layer $\varepsilon^*(\lambda) = \varepsilon_1^*(\lambda) + i\varepsilon_2^*(\lambda)$, with $\varepsilon^*(\lambda) = N^*(\lambda) \times cc[N^*(\lambda)]$ (cc= complex conjugate) will have $\varepsilon_1^*(\lambda) < 0$ if it remains a plasmonic system at wavelengths where the gold itself has $\varepsilon_1^*(\lambda) < 0$. The value of n^* provides information regarding the average phase shifts and effective transit times, while that of k^* reveals details of the average dissipation in the film. We are not aware of any optical studies for such unique film structures apart from a brief preliminary report of our own on one such film [5] whose nanostructure was different to the mesoporous films presented here. We check the internal consistency and physical acceptability of the results with a Kramers-Kronig analysis of the spectrum of n^*, k^* values, because of their unusual spectral character.

II. Experimental details:

A. Film preparation:

Mesoporous gold is made by de-alloying of the intermetallic compound $AuAl_2$ sometimes called "purple gold", in strong NaOH solution. The procedure is as follows:
Alloy films of $AuAl_2$ were prepared by co-depositing the elements using high vacuum dc magnetron sputtering onto glass substrates. The sputtering targets of Au and Al were 99.999% pure discs (50mm diameter), placed 150 mm away from the substrate. The base pressure was better than ~10^{-6} Torr, while sputtering was carried out in the presence of flowing Ar, at a pressure of 3 mTorr. To ensure good homogeneity and crystallinity, a 400°C substrate temperature was used during deposition. In order to get the $AuAl_2$ atomic ratio or correct stoichiometry, the relative atomic densities of the Au and Al targets are taken into account giving a thickness ratio of 10% gold and 90 % Al in terms of relative thickness rates of deposition. For instance in one sample 20 nm of gold equivalent is co-deposited with 160 nm of aluminium equivalent for a 180 nm thick alloy film. If correctly deposited, the film will be purple in colour under white light due to a reflectance minimum in green (about 2.2ev). The $AuAl_2$ absorbs green and hence reflects mainly red and blue to yield a net reflection colour of purple. Minimum thicknesses used were determined by in *situ* electrical measurements on some growing films to ensure electrical continuity [6]. After co-depositing of $AuAl_2$ on a glass substrate, aluminium was removed from the compound by immersing the films in NaOH solution. The residual film consists of mesoporous gold on glass.

B. Microscopy:

Scanning electron microscopy (SEM) with a Schottky Field Emission instrument (LEO) was used to study the nanostructure of the films. Atomic-force microscopy (AFM) with a Digital Instruments IIIA force microscope operating in tapping mode was used to study the surface topography and to accurately determine the thickness of the films. Thicknesses quoted from here on are actual mean thicknesses. Thicknesses given by the crystal monitor during deposition, which is not adjusted, cover a range of densities and are thus a guide to mass deposited. Figure 1 (a) shows typical SEM images of a 20 nm thick mesoporous gold film and Figure 1(b) shows tapping mode AFM images of the

same mesoporous gold film (Scan size: 1μm x 1μm). The SEM imag e clearly shows the porous structure and the inset graph of the image shows more details of the surface using a larger magnification. The pore sizes were measured by analysis of high-resolution SEM images with the assistance of a computer program that superimposed a circle of approximately matching diameter over the pore opening. The results are shown in Figure2. It is evident that pore diameters are in the range 6 to 18 nm, with preponderance at around 12 nm.On the other hand, the AFM scan profile shows the sizes of pores in more details . The internal surface area of the film depends strongly on the size and volume fraction of the pores and the thickness of the film. These topological dimensions and shapes can be changed using various approaches; by varying the mass percent in the alloy of the two deposited materials, by varying the deposition parameters such as power, deposition rates and substrate temperature, or by having a different substrate such as a pre-coating with a thin Cr layer. We reported the nanostructure of a film grown on Cr earlier [7]. The latter has a void structure with more inter-penetrating and internal winding channels than the structure in Figure 1.

C. Optical measurements and data

Two techniques are used to establish the optical response of the specular mesoporous gold films. This data is then used in combination to determine the optical constants of the optically equivalent homogeneous layer that gives the same response as the inhomogeneous layer. The best fit models were obtained using the WVASE32 software for J.A.Woollam Co.,Inc.

(i) *Spectrophotometry*: Specular transmittance *(T)* and reflectance *(R)* of the samples at normal incidence were measured in the range 300-2500nm using a Cary 5E UV-VIS-NIR spectrophotometer, and the absorbance *A (A=1-R-T)* is deduced from them. Experimental data on the optical properties of a mesoporous gold film are compared to a normal thin gold film of the same thickness (~20nm) deposited with the same apparatus in Figure 3 which shows $T(\lambda)$ and $R(\lambda)$ results respectively. The optical set up for the near normal (7°) reflectance measurements in the Cary Spectrophotometer is 'VW'. This means that a "V" path is used for the reference beam while a "W" path applies to the samples. Since the beam in the "W" path is reflected twice from the two different spots on the sample surface several mm apart, the accuracy of the result can be affected by any non-uniformity of the sample. However such effects seem to be small in the present work. Also shown in Figures 3and 4 are the fits obtained with a thin film model of the system using best-fit optical constants at each wavelength (see section III) and the measured thickness. The simple thin film specular model with an equivalent optical layer described by a single pair of refractive indices at each wavelength clearly works very well for all wavelengths except those below 450 nm. This is believed to be due to small non-specular contributions to $R(\lambda)$ at these shorter wavelengths, which are starting to resolve the nanostructure and hence weakly scatter, whereas longer wavelengths interact with it as if it were homogeneous. Even weak scattering will lead to significant errors in attempting to fit optical results with a uniform layer representation.

(ii) *Ellipsometry*: The second optical method uses a UVISEL spectroscopic phase modulated ellipsometer to study the 20 nm thick mesoporous gold film. Prior to spectroscopic scans the back surface of the glass substrate was covered with black tape to eliminate any back-surface reflection entering the detector because the 20nm mesoporous gold layer is not opaque. The spectroscopic scans were performed at different angles of incidence, with respect to the surface normal, between 65º and 75º, at 5º intervals, and wavelengths ranging from 300nm-800nm, with 5nm intervals. In this ellipsometric technique the reflected amplitude ratios (ψ) and relative phase shifts (Δ) for reflected light, which is s- and p-polarized, are directly measured. It is thus in principle more accurate and sensitive than spectrophotometry where the phase shifts enter indirectly in measurement of the absolute intensity of the reflected and transmitted light. The measured values of ψ and Δ are related to the ratio of Fresnel amplitude reflection coefficients r_p and r_s of p- and s-polarized light by the ellipsometry equation ($\rho = r_p/r_s = \tan(\psi)e^{i\Delta}$). The measured values of the ψ and Δ are presented in Figure 4 along with curves generated by a Kramers-Kronig analysis as discussed in section III. Because the ellipsometry data is collected at high angles of incidence, differences may arise in optical constants derived from near normal incidence spectrophotometry (see section iii). One cause could be some anisotropy, but the other and most influential is likely to be the impact of surface plasmons on $R(\lambda)$ and $T(\lambda)$. Surface plasmons can be present if a surface or film is both metallic and nanostructured [7]. The coupling of light to surface plasmons depends on the wave vector component parallel to the interface and hence angle of incidence [8].
The complex optical constants n^*, k^*, and thickness t of the optically equivalent layer, determine R, T, ψ and Δ. They are affected by the sample's physical parameters, including refractive indices and shape of components, composition, component distribution, porosity, layer thickness, and both surface profiles. The details of how radiation is effected by these features are needed to understand the equivalent layer response. We can however determine the optical constants of the layer that is optically equivalent to our mesoporous gold films accurately via beam intensities (Reflectance (R) and Transmittance (T)) or polarization states (ellipsometric ψ and Δ) as a function of the wavelength and angles of incidence of the light beam. Such results can then be used to gain insights into the dominant mechanisms and the systematics of how nanostructure and other geometric changes influence average optical properties.

(iii) *Fitting both ellipsometric and transmittance data at the same angle:* In order to show the influence of the incident angle on the optical indices of mesoporous gold films the spectrophotometer results (T) for the 20 nm mesoporous film at angle 65º were fitted together with ellipsometric ψ and Δ at the same angle using the modelling software. As shown in Figure 5 the least squares fits were excellent for the whole range of wavelengths with a very small mean square error (MSE). Inset graphs of Figure 6show the optical constants n^* and k^* as a function of wavelength and angle of incidence (65º). It is very clear that changing of incidence angle has a greater effect on the refractive index (n^*) than the extinction coefficient (k^*).

III. Analysis and Discussion

Starting with accurately determined average film thickness using AFM we proceeded to determine the best fit complex indices that describe the data. In these procedures a "start" guess is needed for the unknown layer and we start with bulk gold data from Palik [4]. The fitting parameters are thus the real part of refractive index (n^*) and extinction coefficient (k^*) of the uniform layer that is optically equivalent to the mesoporous layer. A simple model of three smooth surface layers the ambient (*Air*), the "unknown" film, and the substrate (Super white glass, for which n, k were obtained separately from our own ellipsometric experimental values fitted with a Cauchy model).

The accuracy, reliability and physicality of the fitted optical constants using both spectrophotometry and ellipsometry can be checked with the classic causality relationship of Kramers-Kronig (K-K) [9]. The requirement of causal nature of the response of a material means electromagnetic waves can not be reflected or absorbed by the material before the arrival of the primary light wave. Therefore, the real and imaginary parts of the complex refractive index $N^*(\omega) = n^*(\omega)+ik^*(\omega)$, and of the complex dielectric function $\varepsilon^*(\omega)=\varepsilon_1^*(\omega)+i\varepsilon_2^*(\omega)$ are not independent quantities. They are related by

$$\varepsilon_1(\omega) = 1 + \frac{1}{\pi} p \int_{-\infty}^{\infty} \frac{\varepsilon_2(\omega')}{\omega' - \omega} d\omega' = 1 + \frac{2}{\pi} p \int_{0}^{\infty} \frac{\omega' \varepsilon_2(\omega')}{\omega'^2 - \omega^2} d\omega', \qquad \textbf{(1)}$$

where p stands for Cauchy principal value of the integral.

Using the modelling software, the spectrophotometer results (R and T) for the 20 nm gold film and the mesoporous film were fitted. The fitting process started with the optical constants of bulk gold material inputted for both unknown layers [4]. The quality of fitting obtained for 20nm gold film on glass is shown in Figure (2) while the fitting for the mesoporous gold layer was also excellent for wavelengths above 450 nm as noted above. However the model gets increasingly inaccurate at shorter wavelengths due presumably to the occurrence of some scattering. An example of the K-K analysis, for the ellipsometric data is shown in Figure 4.

To further gain some insights, the data were fitted using both of the most common and widely used approximations for the complex dielectric permittivity of a two component random medium, namely Maxwell-Garnett, equation 2(a) for $\varepsilon^* = \varepsilon_{MG}$, or the Bruggeman formalism, equation 2(b) for $\varepsilon^* = \varepsilon_{BG}$ [10].

$$\tilde{\varepsilon}_{MG} = \varepsilon_h + 3f\varepsilon_h \frac{\varepsilon_i - \varepsilon_h}{(1-f)\varepsilon_i + (2+f)\varepsilon_h}, \qquad 2(a)$$

$$f \frac{\varepsilon_i - \tilde{\varepsilon}_{BG}}{\varepsilon_i + 2\tilde{\varepsilon}_{BG}} + (1-f) \frac{\varepsilon_h - \tilde{\varepsilon}_{BG}}{\varepsilon_h + 2\tilde{\varepsilon}_{BG}} = 0, \qquad 2(b)$$

where ε_i is the dielectric permittivity of the inclusions in the MG model and ε_h is the dielectric permittivity of the host medium, while in the BG model both have equivalent topology. Using known dielectric parameters of the host and known filling factors (f), the dielectric permittivity ε_i can be extracted as the fitted parameter. Alternately, using known dielectric permittivity of both constituents we can determine the filling factor (f).
Since the gold percolates we use the MG model with gold as host and find reasonable fits with $f_{Au} = 0.11$, and voids represented as inclusions with $f_{Void}=0.89$. (The filling factor values were determined by using the weight percentage of the two material*s*). The substrate is glass. The depolarization factor, which describes the shape of the constituents in the EMA mixture is not included in above equation because it does not make any difference in the fitting and as a parameter it can also link to inclusion correlation effects, therefore it was deemed best to fix it at the value of 0.333, corresponding to spheres. An additional EMA layer to allow for extra surface roughness did not improve the quality of the fit. For example an EMA layer (f_{Au}=50% and f_{Void}=50% with fitted thickness=1nm) added as a surface roughness layer did not reduce the mean square error (MSE) [11] sufficiently to be significant. Thus we retained the single layer model.
Fitting ellipsometry data across a wide spectrum for three incident angles increases the reliability and accuracy. The best fit model was taken as that which minimized the MSE. The complex refractive index $N^* = n^*+ik^*$, where the real part (n^*) determines the phase shift of the propagating wave in the material and the phase velocity ($v_{phase} = \omega/k$) while the imaginary part (k^*) determines the attenuation of the amplitude of the propagating wave in the medium. They are related to the complex dielectric function by the relation $\varepsilon^*(\lambda) = N^*(\lambda) \times cc[N^*(\lambda)]$. Figure 4 shows the fitting of the experimentally determined ellipsometric parameters for a 20 nm mesoporous gold film on glass. The same methods have been applied for the conventional thin gold film.
Ellipsometry is highly accurate and sensitive for very thin films such as our mesoporous gold layers. It supplies phase and amplitude information at a range of angles of incidence, but ellipsometric data can be difficult to interpret at higher angles of incidence in many instruments. Reflectance measurements combine effects of phase and amplitude into intensity. However, they are straightforward at near-normal incidence. Also, absolute intensity measurements are effected by fluctuations in source intensity and partial scattering from the surface. Therefore, in order to determine if the fit parameters have physically acceptable dispersion, the results must comply with the Kramers-Kronig criterion. It is wise to check this when anomalous behaviour such as is apparent here, is observed. The striking feature, as seen in Figure 3, of the transmittance and reflectance of the mesoporous gold film are that they are nearly independent of wavelength in the NIR range 2500 nm > λ > 800nm, while for the conventional 20 nm thick thin gold film they are still changing noticeably at these NIR wavelengths. The dielectric constants found from fitting R and T together in the above range were found to satisfy the K-K relation in equation (1) so that the optical constants obtained for the range above $\lambda \geq 800$ nm can be relied on for both samples.
Ellipsometric results as in Figures 4 and 5were acquired only in the range 300 nm $\leq \lambda \leq$ 800nm due to spectral limitation in the instrument used. Results for refractive index and extinction coefficient for both samples are presented in Figure 6 and were found from combining ellipsometry and transmittance data in a single fit. They also satisfy the KK relations.

Inset graphs of Figure 6 show the optical constants n^* and k^* as a function of wavelength and angle of incidence (65º). It is very clear that changing of incidence angle has a greater effect on the refractive index (n^*) than the extinction coefficient (k^*). At longer wavelengths (using spectrophotometry only) k^* at 0° and 65° match but n^* does not. The results verify what we predicted in earlier work for different metal nanostructures, namely that equivalent layer optical constants would change as angles of incidence varied [5] due to surface plasmon coupling across the layer.
The usual pronounced linear increase with wavelength in the k^* value above 500nm, for the 20nm gold film is associated with the Drude free electron response of gold. In contrast the 20 nm mesoporous gold film shows a weakly linear rise in k^* and a much lower value in the range 1 to 2 compared with 1 to 9 as seen in Figure 4 for bulk gold. Thus as wavelength increases, the relative attenuation of the two materials diverges rapidly. This qualitative and quantitative shift is linked to the mesoporous film containing a continuous network of nanoscale pores and channels. The refractive index shows that the 20nm gold film is similar in behaviour to the bulk gold film data but the distinct shift due to the thicknesses and the structural differences of 20 nm gold film also has n^* less than 1 in the range shown, which is typical metal-like behaviour. In contrast, the 20nm mesoporous gold film has a large n^* and is almost insulator like but even differs from an insulator in that the reflectance spectrum is nearly flat for the range above $\lambda \geq 800$nm as shown in Figure 3. Some borderline metallic behaviour is apparent in the effective indices in the shape of the n^* and k^* curves and the broadband medium value of k^*, which is not usual in insulators. Effectively it is barely or very weakly plasmonic. We can thus say that mesoporous metal films exhibit distinct and unique optical behaviour which is neither metal or insulator like and unique in its spectral flatness, the bandwidth over which this occurs, and the magnitudes of the effective optical constants over these wavelengths. Such unique response means new optical applications may be enabled by these systems.

As shown above, the arbitrary pore sizes playing important role on the optical properties of the mesoporous gold films. We should point out that we expect another unique optical responses if the pores made in regular shapes, sizes, and distances.

IV. Conclusion

Very thin mesoporous gold films on glass substrates were produced for the first time, and the optical properties were explored and compared with dense gold films of the same thickness. Ellipsometric and spectrophotometric methods were used to study optical properties and to extract optical constants for the equivalent uniform homogeneous layer. Good agreement between the fitted model and experimental results were obtained except for the reflectance of the mesoporous film for the range $\lambda \leq 450$nm where a small amount of scattering may be present. We also found that changes in the angle of incidence have a strong impact on the refractive index (n^*) but not on the extinction coefficient (k^*).
Mesoporous gold films exhibit unique dispersion in their optical response across all NIR wavelengths. The effective optical constants as a function of wavelength, which are physically acceptable from a dispersion viewpoint, are neither metal- nor insulator-like. This is in effect a quite new class of optical material.

ACKNOWLEDGMENT

We are grateful to Geoff McCredie for his excellent technical support for thin film preparations and help with the ellipsometry measurements. The assistance of colleagues at UTS Microstructural Analysis Unit with the high-resolution SEM studies and AFM is also gratefully acknowledged.

References:

[1] Cortie,M.B., Van der Lingen,E. and Pattrick, G. Catalysis and capacitance on nanostructured gold particles and sponges, *APNF 2003 - Oz Nano 03*, Cairns, 19-21st November 2003, 2004 World Scientific, Singapore 79
[2] Kamijyou K1997 *Metals and Technology (Japan)* **67(1)** 38
[3] M. B. Cortie, A.I. Maaroof, and G. B. Smith [Submitted to Gold Bulletin]
[4] Palik E D (ed.) 1998 *Handbook of Optical Constants of Solids* vol I (San Diego, CA: Academic Press)
[5] Smith G B, and Maaroof A I 2004 Opt. Commun. (Article in Press, available online)
[6] Maaroof AI, and Evans B L 1994 J. Appl. Phys. **76(2)** 1047
[7] Smith G B, Maaroof A, Allan R, Schelm S, Anstis G, and Cortie MB 2004 SPIE **V.4** 5508
[8] Raether H 1988 Surface Plasmons on Smooth and Rough Surfaces and on Gratings Tracts in Modern Physics**Vol.111** (Springer, Berlin)
[9] Wooten F 1972 Optical Properties of Solids (Academic Press)
[10] Aspnes D E 1982 Thin Solid Films **89** 249
[11] Azzam R M A, and Bashara N M 1977 Ellipsometry and Polarized Light (North Holland Press, Amsterdam)

Figures Caption:

Figure 1 (a): SEM image taken at magnificationX100000 while the inset image at X188000 of the 20nm mesoporous gold film.

Figure 1 (b): Tapping mode AFM image of 20nm mesoporous gold film (scan size: 1μm×1μm) and the inset graph shows the profile of the mesoporous structure.

Figure 2 : Pore size distribution of 20nm mesoporous gold film on glass substrate.

Figure 3: Spectrometric data of spectral transmittance and reflectance at normal incidence for 20nm normal thin film gold and mesoporous gold film on glass substrate.

Both experimental (markers) and modeled (solid line) data are shown. The inset graph shows Absorptance deduced from $A=1-R-T$.

Figure 4: Ellipsometric data ψ and Δ obtained for 20nm mesoporous gold film on glass substrate for three angles of incidence. Both experimental (markers) and modeled (solid line) data are shown.

Figure 5: Spectrometric and ellipsometric data at angle of incidence 65º for 20nm mesoporous gold film on glass substrate.

Figure 6: Optical constants n^* and k^* as a function of wavelength for 20nm gold film and 20nm mesoporous gold film on glass substrate obtained from fitting spectrophotometry data in Figure 2, the bulk data from Palik [4] for comparison. Inset graphs shows the optical constants n^* and k^* as a function of wavelength and one angle of incidence (65º) for 20nm mesoporous gold film on glass substrate obtained from fitting ellipsometric data with and without spectroscopic Transmittance at 65º.

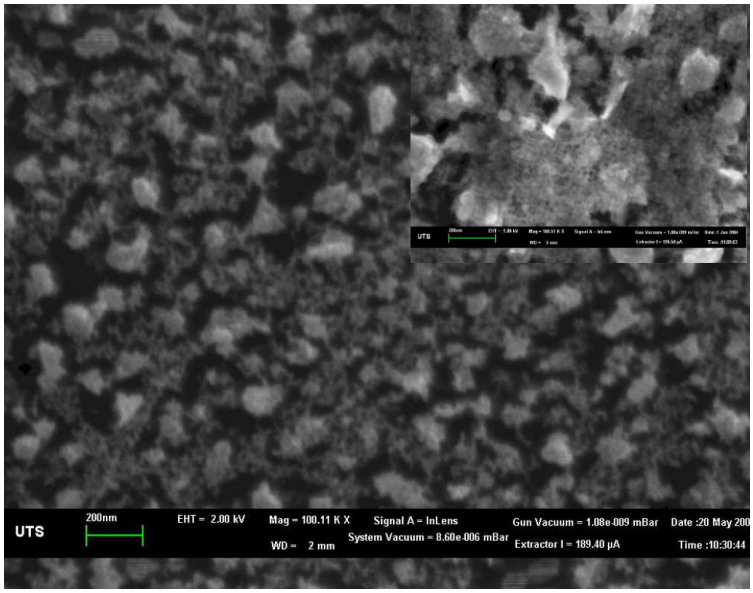
UTS
200nm
EHT = 2.00 kV
Mag = 100.11 K X
Signal A = InLens
WD = 2 mm
System Vacuum = 8.60e-006 mBar
Gun Vacuum = 1.08e-009 mBar
Extractor I = 189.40 µA
Time :10:30:44

Fig 1a

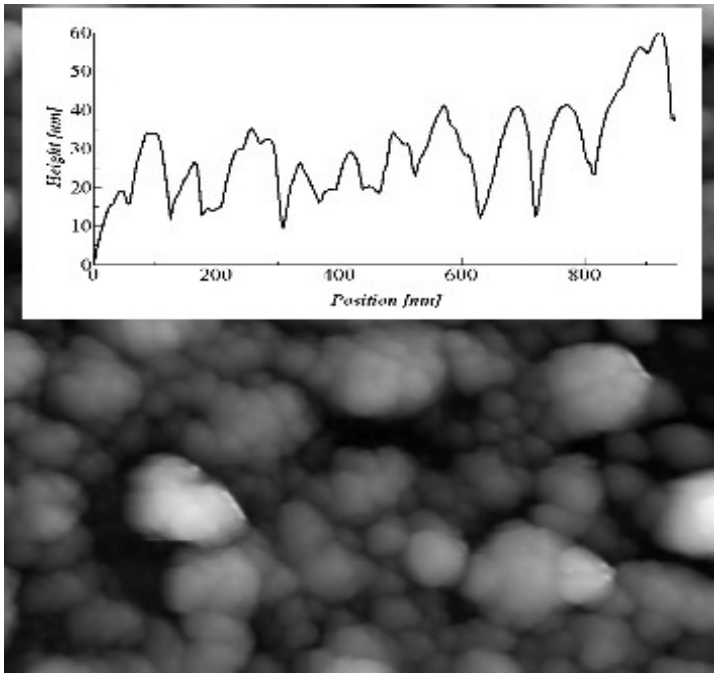

Fig1b

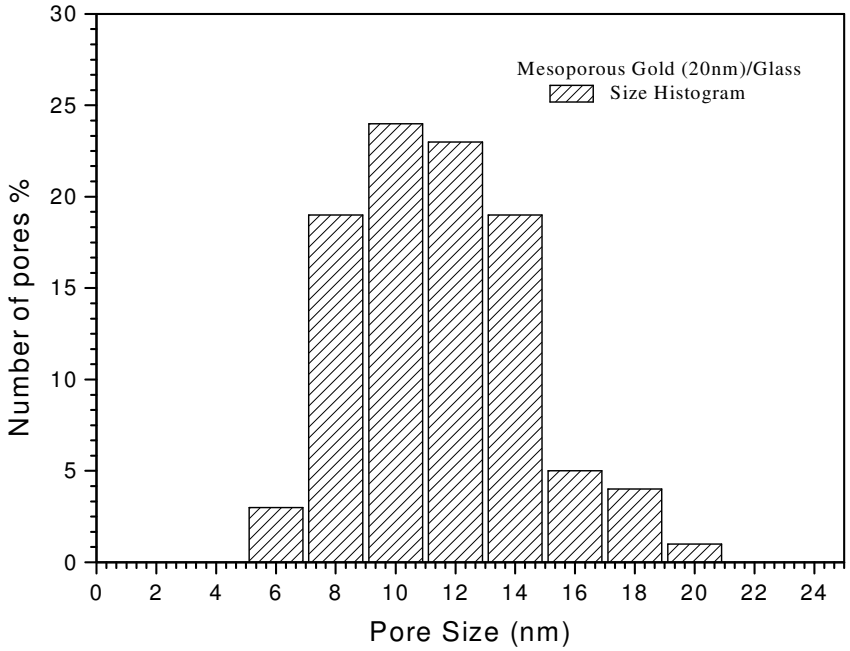
Mesoporous Gold (20nm)/Glass
Size Histogram
Number of pores %
Pore Size (nm)
0
5
10
15
20
25
30
0
2
4
6
8
10
12
14
16
18
20
22
24

Fig.2

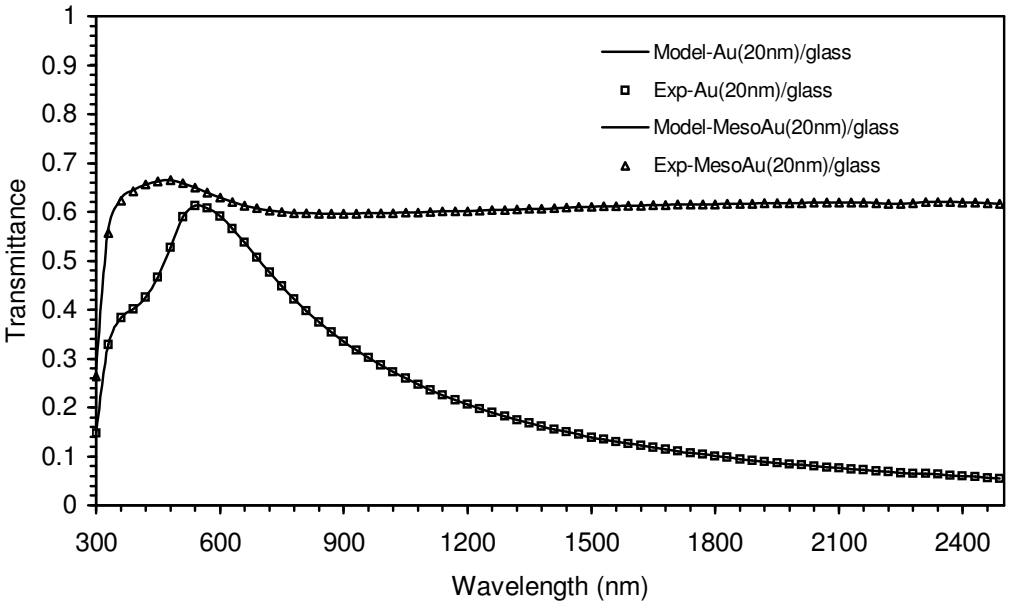
Model-Au(20nm)/glass
Exp-Au(20nm)/glass
Model-MesoAu(20nm)/glass
Exp-MesoAu(20nm)/glass
Transmittance
Wavelength (nm)

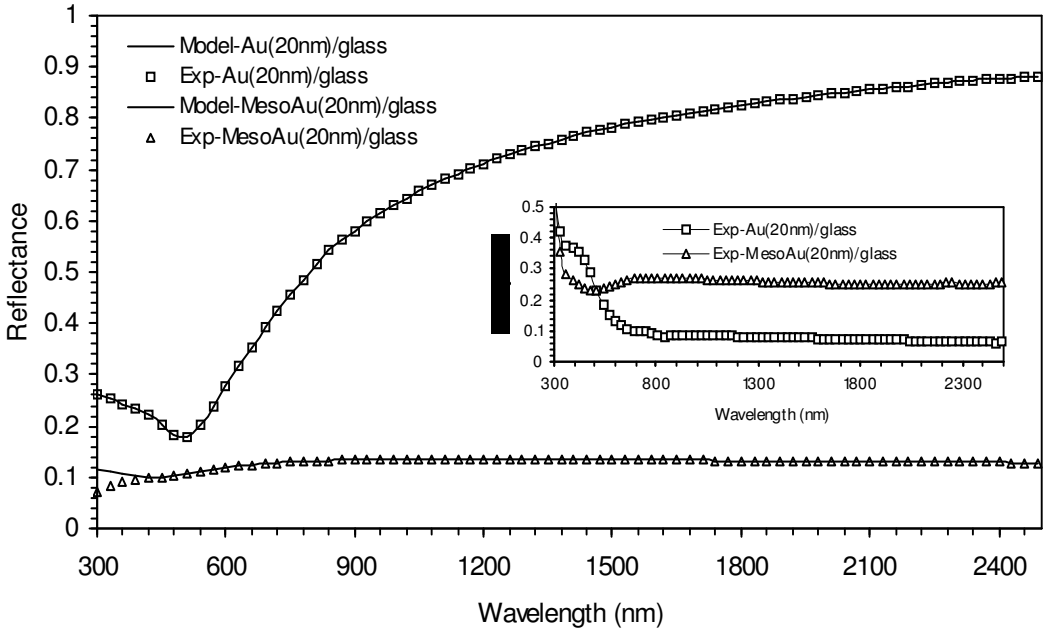
Model-Au(20nm)/glass
Exp-Au(20nm)/glass
Model-MesoAu(20nm)/glass
Exp-MesoAu(20nm)/glass
Reflectance
Wavelength (nm)
Exp-Au(20nm)/glass
Exp-MesoAu(20nm)/glass
Wavelength (nm)

Fig3

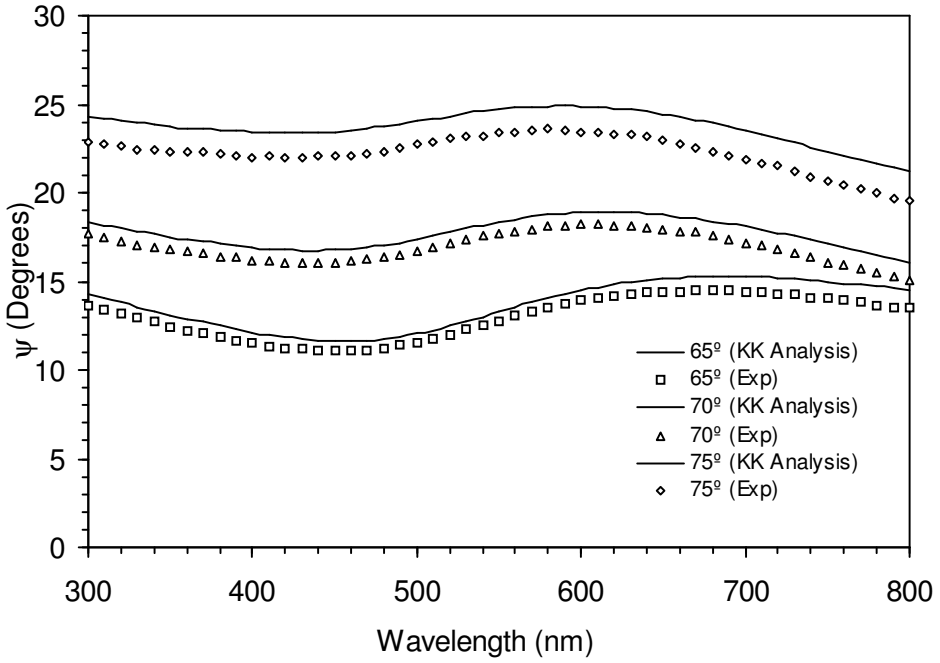
30
25
20
15
10
5
0
ψ (Degrees)
300
400
500
600
700
800
Wavelength (nm)
65º (KK Analysis)
65º (Exp)
70º (KK Analysis)
70º (Exp)
75º (KK Analysis)
75º (Exp)

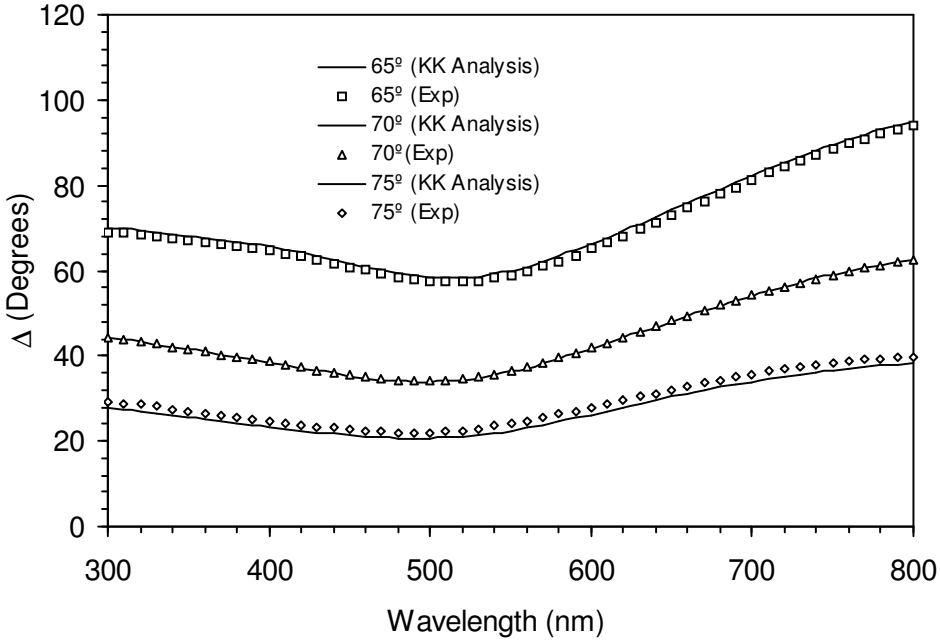
120
100
80
60
40
20
0
Δ (Degrees)
300
400
500
600
700
800
Wavelength (nm)
65º (KK Analysis)
65º (Exp)
70º (KK Analysis)
70º(Exp)
75º (KK Analysis)
75º (Exp)

Fig4

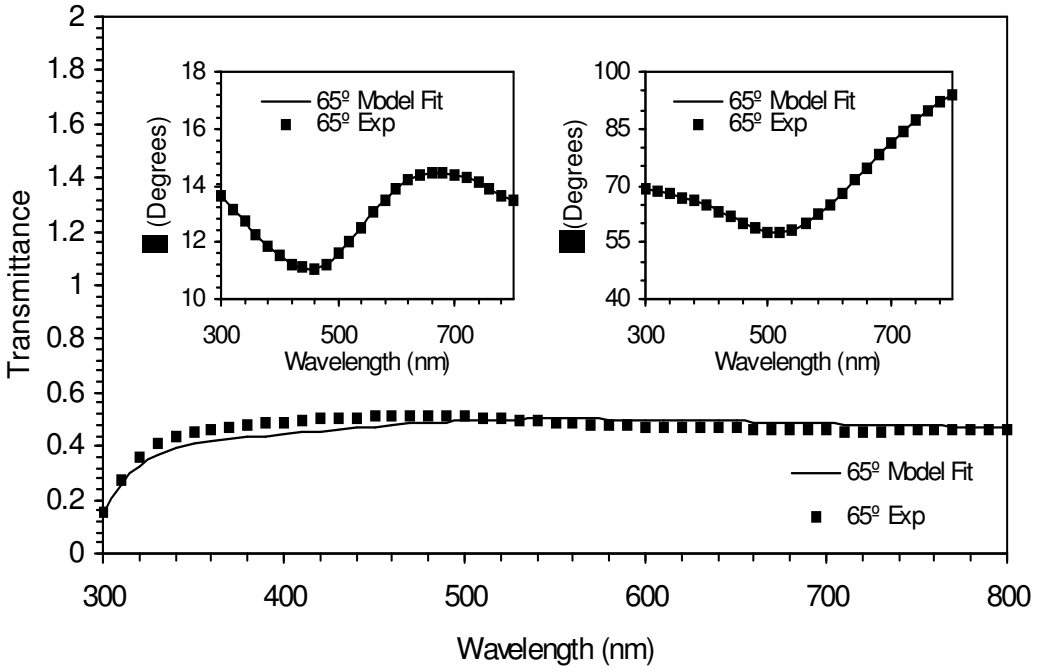
Transmittance
Wavelength (nm)
65º Model Fit
65º Exp
(Degrees)
Wavelength (nm)
65º Model Fit
65º Exp
(Degrees)
Wavelength (nm)
65º Model Fit
65º Exp

Fig 5

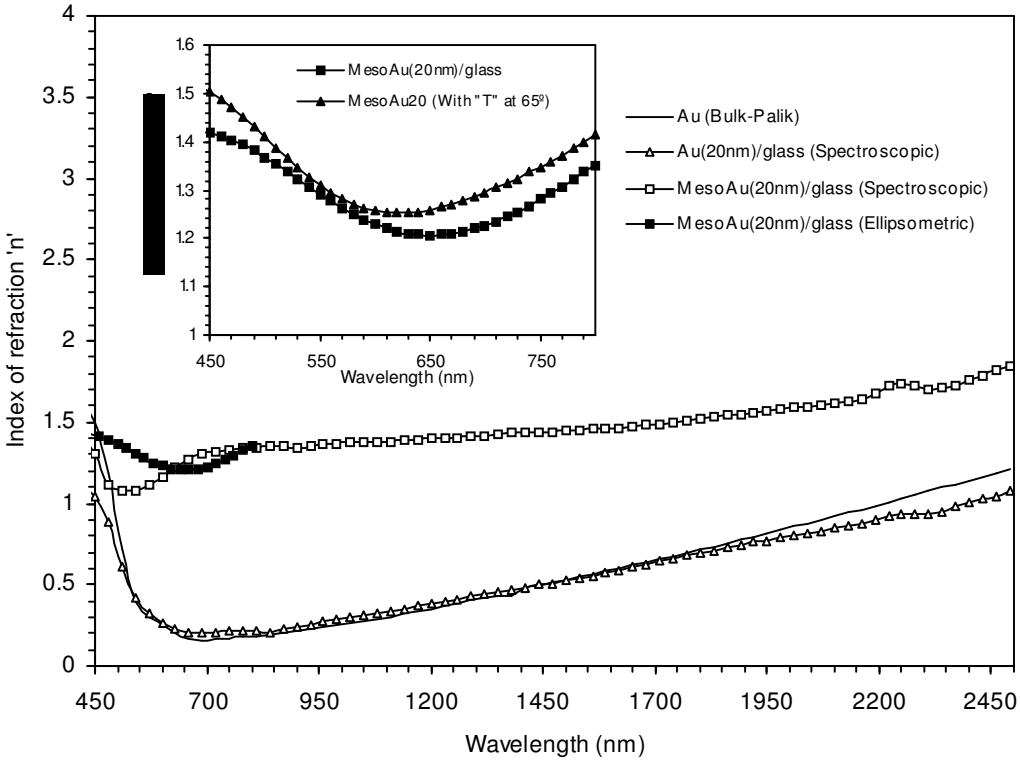
Index of refraction 'n'
Wavelength (nm)
MesoAu(20nm)/glass
MesoAu20 (With "T" at 65º)
Au (Bulk-Palik)
Au(20nm)/glass (Spectroscopic)
MesoAu(20nm)/glass (Spectroscopic)
MesoAu(20nm)/glass (Ellipsometric)

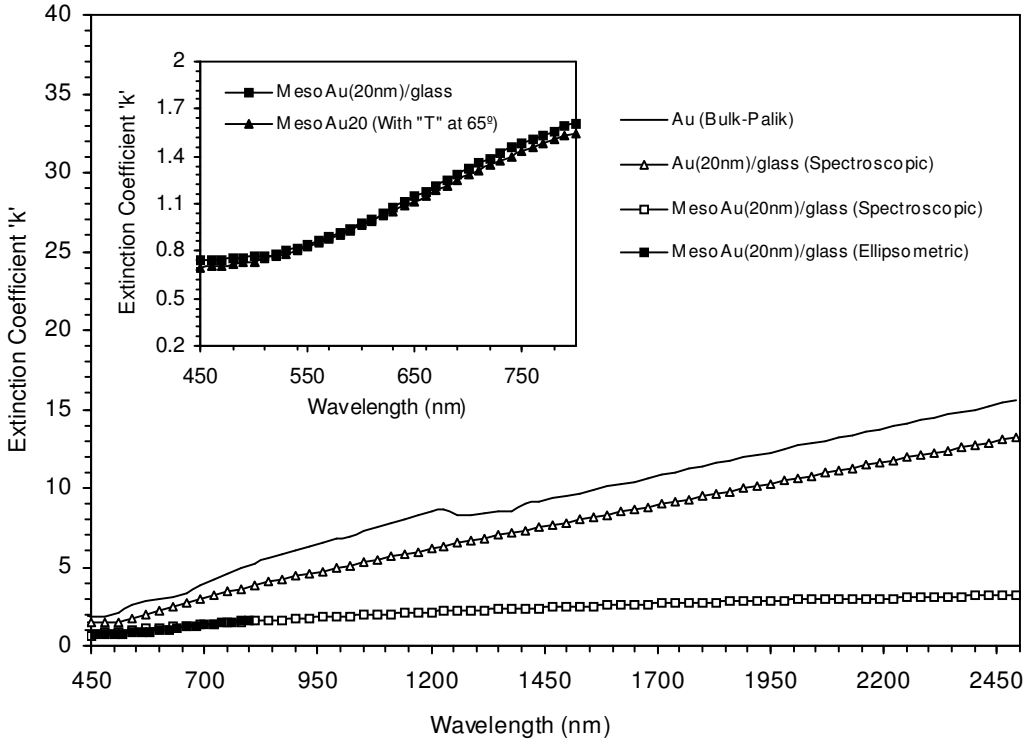
Extinction Coefficient 'k'
Wavelength (nm)
MesoAu(20nm)/glass
MesoAu20 (With "T" at 65º)
Au (Bulk-Palik)
Au(20nm)/glass (Spectroscopic)
MesoAu(20nm)/glass (Spectroscopic)
MesoAu(20nm)/glass (Ellipsometric)

Fig6